The Effects of Digital Cameras Optics and Electronics for Material Acquisition

N. Holzschuch[1] and R. Pacanowski[2]

[1]Inria ; Univ. Grenoble Alpes, LJK ; CNRS, LJK
[2]LP2N (CNRS) – Université de Bordeaux

Abstract

For material acquisition, we use digital cameras and process the pictures. We usually treat the cameras as perfect pinhole cameras, with each pixel providing a point sample of the incoming signal. In this paper, we study the impact of camera optical and electronic systems. Optical system effects are modelled by the Modulation Transfer Function (MTF). Electronic System effects are modelled by the Pixel Response Function (PRF). The former is convolved with the incoming signal, the latter is multiplied with it. We provide a model for both effects, and study their impact on the measured signal. For high frequency incoming signals, the convolution results in a significant decrease in measured intensity, especially at grazing angles. We show this model explains the strange behaviour observed in the MERL BRDF database at grazing angles.

1. Introduction

When acquiring materials and reflectance, the first step is to take pictures of material samples; these samples are usually spheres, cylinders or flat samples. The acquisition process takes pictures under varying lighting conditions and camera orientations, and combines them into a measured material response, such as a BRDF. Replacing non-imaging devices with cameras resulted in a significant acceleration for acquisition time.

The pictures taken by digital cameras are arrays of pixels, with their positions and intensity. For convenience, we usually treat the digital cameras as perfect pinhole cameras, and the pixels as point samples of the incoming signal, neglecting the impact of the camera optical and electronic system. The effects of the optical system are modelled by the Modulation Transfer Function (MTF), which is convolved with the incoming signal. The effects of the electronic system are modelled by the Pixel Response Function, which is multiplied with the signal, after convolution by the MTF. The product is integrated over the pixel sensor.

The MTF acts as a low-pass filter, lowering the frequency of the incoming signal. The filter width depends on the orientation of the surface being photographed. It becomes quite large at grazing angles, and has an impact on the measured intensity. The PRF effects are more subtle.

For materials with high-frequency content relative to the Modulation Transfer Function, the net result is a significant decrease in measured intensity, especially large at grazing angles. For spherical samples of quasi-specular materials, it corresponds to an extra multiplication $\cos\theta_o$. This explains the strange behaviour observed in some BRDFs of the MERL database at grazing angles.

2. Previous work

Acquiring material reflectance is a tedious process, requiring sampling at all incoming and outgoing directions. Marschner et al. [MWLT00] used spherical samples to speed-up the acquisition process for isotropic materials: a single picture captures all outgoing directions. Matusik et al. [MPBM03] and Matusik [Mat03] extended this approach and acquired BRDF samples from 100 different materials, creating the MERL BRDF database.

Ngan et al. [NDM05] extended the approach to cylinders for anisotropic materials, and compared the behaviour of measured BRDFs with model predictions. At grazing angles, measured values in the MERL database are significantly lower than what reflectance models predict. Later researchers (e.g. Bagher et al. [BSH12]) discarded the data at grazing angles, avoiding the issue.

Bagher et al. [BSN16] showed that they could reconcile measured data with the Cook-Torrance micro-facet model [CT82] if they used the shadowing function as a free parameter, instead of using the Smith shadowing term [Smi67].

Holzschuch and Pacanowski [HP17] studied the impact of the MERL acquisition apparatus on the measured signal. They showed that a convolution by a camera filter could explain the strange behaviour of the MERL database at grazing angles, although they attributed this convolution to the Pixel Response Function. We show that two different phenomenon are responsible: the camera optics through the Modulation Transfer Function, and the camera electronics through the Pixel Response Function.
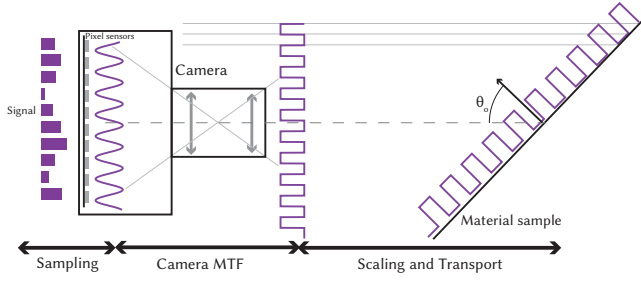
Figure 1: *Our camera model: Incoming signal from the sample is first transported, then convolved by the Camera Modulation Transfer Function, and finally integrated on the sensor pixels.*

Figure 2: *Using spherical samples, position relative to the camera axis x is connected to the angle θ_o: $x = r_S \sin \theta_o$.*

3. Our Camera Model

We consider a material sample and a digital camera, taking pictures of the sample (see Figure 1). The optical axis of the camera is at an angle θ_o from the normal of the sample. We assume that the entire material sample is in focus. To avoid *geometric* distortions by the camera optics (barrel, pincushion), we focus on a sensor area close to the camera axis [MWLT00, Mat03]. This reduces the image effective resolution; for example, on a 1024×1024 pixels sensor, we only use a 512×512 pixels area in the center.

The effects of the camera optics are complex. The Modulation Transfer Function (MTF) is a convenient model [Goo04, chap. 6], encapsulating all of them in a single function, slightly blurring the incoming signal. The signal reaching the camera is convolved by the Modulation Transfer Function. The result of the convolution reaches the sensor. Pixel response is either included in this Modulation Transfer Function or modelled separately using the Pixel Response Function.

The Modulation Transfer Function encodes all the effects of the camera optics. It is represented as a point spread function. The higher the quality of the optics, the smaller the size of the spread. We approximate it using a Gaussian, G_{MTF}, with standard deviation σ_{MTF}. The PRF for pixel p, r_p has a finite support $[x_p - \sigma_p; x_p + \sigma_p]$, where x_p is the position of the pixel centroid. The actual filter can be anything, for example a box function or a windowed Gaussian. $2\sigma_p$ must be smaller than the distance between two pixels.

We write $S(x)$ the incoming signal on the camera sensor, where x is the position relative to the optical axis of the camera. The signal after modulation by the MTF is $S_m(x)$:

$$S_m(x) = \int_{-\infty}^{\infty} S(t - x_p) G_{\mathrm{MTF}}(t)\, \mathrm{d}t = (S * G_{\mathrm{MTF}})(x) \quad (1)$$

If we model the Pixel Response Function separately, the signal $R(x_p)$ recorded at each point of the pixel sensor is the integral of the product of this signal and the PRF:

$$R(x_p) = \int_{x_p - \sigma_p}^{x_p + \sigma_p} S_m(t - x_p) r_p(t)\, \mathrm{d}t = (S_m * r_p)(x_p) \quad (2)$$
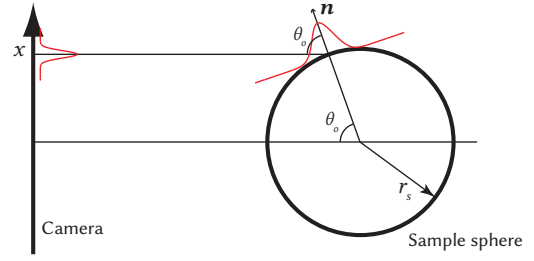
4. Application to Material Acquisition

4.1. Flat Textured Samples

For flat, textured material samples, the signal measured depends on position y on the sample. y is correlated with position on the sensor, depending on the outgoing angle:

$$x = y \cos \theta_o \quad (3)$$

If our sample has reflectance $\rho(y, \boldsymbol{i}, \boldsymbol{o})$, convolved signal is:

$$S_m(x) = \int_{-\infty}^{\infty} \rho\left(\frac{t}{\cos \theta_o} - x_p, \boldsymbol{i}, \boldsymbol{o} \right) G_{\mathrm{MTF}}(t)\, \mathrm{d}t \quad (4)$$

4.2. Spherical Samples

If the material sample is a sphere of radius r_S, position on the camera sensor is connected with outgoing angle θ_o (see Figure 2):

$$x = r_S \sin \theta_o \quad (5)$$

Approximating the sphere by its tangent plane around the position corresponding to the center of the pixel, we get an equation similar to Equation 3:

$$t \approx r_S \cos \theta_o (\theta - \theta_o) \quad (6)$$

$$\theta \approx \theta_o + \frac{t}{r_S \cos \theta_o} \quad (7)$$

This lets us express the convolved signal as a function of the BRDF $\rho(\boldsymbol{i}, \theta)$:

$$S_m(x) = \int_{-\infty}^{\infty} \rho\left(\boldsymbol{i}, \theta_o + \frac{t}{r_S \cos \theta_o} \right) G_{\mathrm{MTF}}(t)\, \mathrm{d}t \quad (8)$$

4.3. Consequence for Measured Signal

For both flat textured samples and uniform spherical samples, the camera records a convolution between the signal we want to measure and the MTF. The incoming signal is scaled internally by a $1 / \cos \theta_o$ factor before the convolution.

For visualisation, we assume the incoming signal is a single peak. If its width is much larger than the width of the MTF Modulation, the convolution is mostly a pass-through (see Figure 3) except at grazing angles. If its width is comparable or smaller than the width of the MTF, the result of the convolution is more dramatic (see Figure 4). There is a significant decrease in maximum intensity *and*
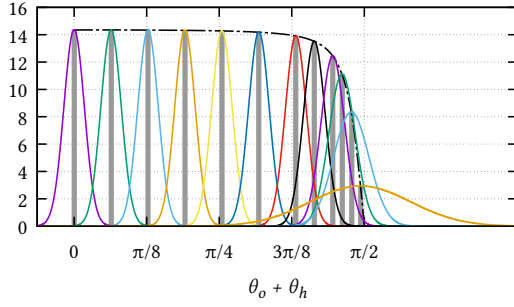
Figure 3: *For a low-frequency signal, convolution by the MTF leaves the signal unchanged, except at grazing angles (input signal: Gaussian, standard deviation = $10 \times \sigma_{MTF}$.) Measured intensity at each pixel is the integral of product between this convolution and Pixel Response Function (PRF, area under gray rectangles).*
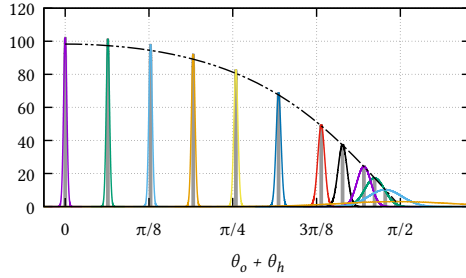
Figure 4: *If the signal frequency is comparable or larger than that of the MTF, convolution by the MTF results in strong reduction in intensity, even at small angles (input signal: Gaussian, standard deviation = σ_{MTF}.) Measured intensity at each pixel is the integral of product between this convolution and Pixel Response Function (PRF, area under gray rectangles).*

signal frequency. The decrease in maximum intensity happens at all directions except normal incidence.

The measured intensity at each pixel is the integral of the product between the convolved signal and the Pixel Response Function (see Figures 3 and 4). The effects are less dramatic. The combined effect is a reduction in measured signal intensity that depends on angle θ_o and incoming signal frequency.

If we assume the measured signal is a Gaussian, the effects depend on its standard deviation compared to that of the Modulation Transfer Function: if it is larger than $100 \times \sigma_{MTF}$ effects are negligible (see Figure 5). If its standard deviation is smaller than $\sigma_{MTF}/10$, reduction in intensity is almost equivalent to an extra multiplication by $\cos\theta_o$.

4.4. Closed Form Expression

When the measured signal is a Gaussian, with standard deviation σ, we have a closed form expression for the impact of camera optics and electronics. The signal after convolution by the MTF is also a
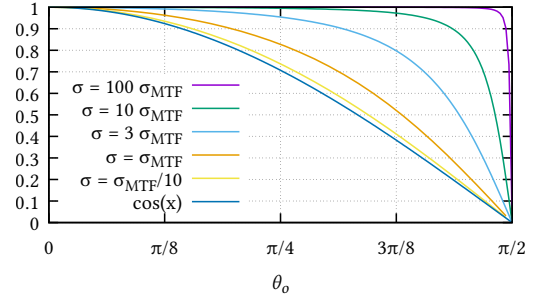
Figure 5: *Reduction in measured intensity depends on frequency of measured signal. We assume the measured signal is a Gaussian, of standard deviation σ.*

Gaussian, with standard deviation σ_m:

$$S_m(x) = \frac{1}{\sqrt{2\pi}\sigma_m} e^{-\frac{x^2}{2\sigma_m^2}} \tag{9}$$

$$\text{where } \sigma_m = \sqrt{\sigma^2 + \frac{\sigma_{MTF}^2}{r_S^2 \cos^2\theta_p}} \tag{10}$$

Assuming a box PRF, the maximum intensity recorded at each pixel is:

$$R(x_p) = \int_{-\sigma_p}^{\sigma_p} S_m(t)\, dt = \operatorname{erf}\left(\frac{\sigma_p}{\sqrt{2}\sigma_m}\right) \tag{11}$$

This can be applied to a Cook-Torrance BRDF model, with a Gaussian distribution. For other distributions (GGX, EPD), there are no closed form expressions. We precompute the intensity decrease as a function of the distribution parameters.

4.5. Application to the MERL BRDF database

Matusik [Mat03] gives detailed information about the acquisition process used for the MERL BRDF database. The digital camera (QImaging Retiga 1300), had a resolution of 1300×1030. Assuming the sample spheres covered half of the image height to avoid lens distortions, sphere pictures have a diameter of ≈ 512 pixels. This gives $\frac{2r_S}{2\sigma_p} = 512$, or $\sigma_p/r_S = 1/512$. We assume that $\sigma_{MTF} \approx \sigma_p$: the quality of the lens is equal to the quality of the sensor.

We consider materials in the MERL database with little or no diffuse component, such as metals (chrome, steel, ss440...). We assume their BRDF follows the Cook-Torrance model:

$$\rho(\boldsymbol{i}, \boldsymbol{o}) = \frac{F(\theta_d)D(\theta_h)G(\boldsymbol{i}, \boldsymbol{o})}{4\cos\theta_i \cos\theta_o} \tag{12}$$

Focusing on the specular peak ($\theta_h = 0$) allows us to extract the Fresnel term F as a function of the measured data:

$$F(\theta_o) = \frac{4\rho(\boldsymbol{i}, \boldsymbol{o})\cos^2\theta_o}{D(0)G(\boldsymbol{i}, \boldsymbol{o})} \tag{13}$$

Although we don't know the value of $D(0)$, assuming G is roughly constant (a reasonable expectation for smooth materials), F should be proportional to $\rho(\boldsymbol{i}, \boldsymbol{o})\cos^2\theta_o$.

(a) `tungsten-carbide`

(b) `chrome-steel`
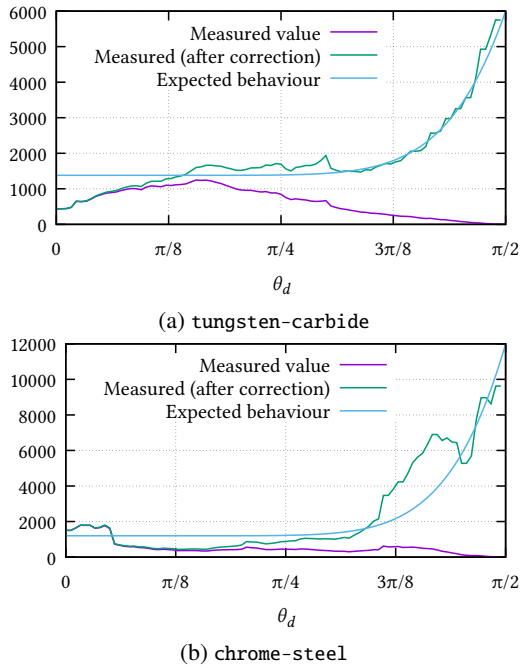
Figure 6: *Extracting the Fresnel term from measured values, we get a function behaving very differently from theory predictions. Taking into account intensity loss caused by the digital camera, we obtain a function whose behaviour is closer to predictions.*

Plotting this value gives a function whose behaviour is *very* different from the expected behaviour of a Fresnel term (see Figure 6). This was first noticed by Ngan et al. [NDM05]. Taking into account the loss in measured intensity caused by the acquisition apparatus computed in Section 4.3, we get a value for the Fresnel term that is closer to the expected behaviour. For specular materials, the divergence occurs quickly, around $\theta > \pi/4$.

5. Conclusion

Digital cameras allow efficient material acquisition. However, inner imperfections of the camera can result in signal distortion during the acquisition process. In this paper, we used a very approximate model for a digital camera, and show that it results in a significant decrease in measured intensity for specular BRDFs. The predictions of our model correspond to the effects observed in the MERL BRDF database.

Taking pictures of regular lines or grids, it is possible to reconstruct the Modulation Transfer Function of a specific camera. We suggest new acquisition apparatus should include this as a preliminary step, and provide it along with the data. Knowing the Modulation Transfer Function and Pixel Response Function, it is possible to compensate for some of the signal distortion introduced, but not all of it.

References

[BSH12] Bagher M. M., Soler C., Holzschuch N.: Accurate fitting of measured reflectances using a Shifted Gamma micro-facet distribution. *Computer Graphics Forum 31*, 4 (June 2012). doi:10.1111/j.1467-8659.2012.03147.x. 1

[BSN16] Bagher M. M., Snyder J., Nowrouzezahrai D.: A non-parametric factor microfacet model for isotropic BRDFs. *ACM Trans. Graph. 36*, 5 (2016). doi:10.1145/2907941. 1

[CT82] Cook R. L., Torrance K. E.: A reflectance model for computer graphics. *ACM Trans. Graph. 1*, 1 (1982), 7–24. doi:10.1145/357290.357293. 1

[Goo04] Goodman J. W.: *Introduction to Fourier Optics*, 3rd ed. W. H. Freeman, 2004. 2

[HP17] Holzschuch N., Pacanowski R.: A Two-Scale Microfacet Reflectance Model Combining Reflection and Diffraction. *ACM Transactions on Graphics 36*, 4 (Aug. 2017), 12. Article 66. doi:10.1145/3072959.3073621. 1

[Mat03] Matusik W.: *A Data-Driven Reflectance Model*. PhD thesis, Massachusetts Institute of Technology, Sept. 2003. Adviser: L. McMillan. URL: http://people.csail.mit.edu/wojciech/pubs/phdthesis.pdf. 1, 2, 3

[MPBM03] Matusik W., Pfister H., Brand M., McMillan L.: A data-driven reflectance model. *ACM Trans. Graph. 22*, 3 (2003). doi:10.1145/882262.882343. 1

[MWLT00] Marschner S. R., Westin S. H., Lafortune E. P. F., Torrance K. E.: Image-based bidirectional reflectance distribution function measurement. *Appl. Opt. 39*, 16 (Jun 2000), 2592–2600. doi:10.1364/AO.39.002592. 1, 2

[NDM05] Ngan A., Durand F., Matusik W.: Experimental analysis of BRDF models. In *Eurographics Symposium on Rendering* (2005). doi:10.2312/EGWR/EGSR05/117-126. 1, 4

[Smi67] Smith B.: Geometrical shadowing of a random rough surface. *IEEE Transactions on Antennas and Propagation 15*, 5 (Sept. 1967). doi:10.1109/TAP.1967.1138991. 1